Original research paper

Mutation of *OUR1*/*OsbZIP1*, which encodes a member of the basic leucine zipper transcription factor family, promotes root development in rice through repressing auxin signaling

Tomomi Hasegawa[a], Nonawin Lucob-Agustin[a,b], Koki Yasufuku[a], Takaaki Kojima[a], Shunsaku Nishiuchi[a], Atsushi Ogawa[c], Misuzu Takahashi-Nosaka[d], Mana Kano-Nakata[e], Mayuko Inari-Ikeda[e], Moeko Sato[f], Hiroyuki Tsuji[f], Cornelius Mbathi Wainaina[e,g], Akira Yamauchi[a], Yoshiaki Inukai[e*]

[a] Graduate School of Bioagricultural Sciences, Nagoya University, Nagoya, Aichi, 464-8601, Japan

[b] Philippine Rice Research Institute, Central Experiment Station, Science City of Muñoz, Nueva Ecija, 3119, Philippines

[c] Department of Biological Production, Akita Prefectural University, Akita, Akita, 010-0146, Japan

[d] National Institute of Genetics, Mishima, Shizuoka, 411-8540, Japan

[e] International Center for Research and Education in Agriculture, Nagoya University, Nagoya, Aichi, 464-8601, Japan

[f] Kihara Institute for Biological Research, Yokohama City University, Yokohama, Kanagawa 244-0813, Japan

[g] Department of Horticulture and Food Security, Jomo Kenyatta University of Agriculture and Technology, Nairobi, 00200, Kenya

*: Corresponding author.

inukaiy@agr.nagoya-u.ac.jp (Y. Inukai)

Abstract

A well-developed root system is essential for efficient water uptake, particularly in drought-prone environments. However, the molecular mechanisms underlying the promotion of root development are poorly understood. We identified and characterized a rice mutant, *outstanding rooting1* (*our1*), which exhibited a well-developed root system. The *our1* mutant displayed typical auxin-related phenotypes, including elongated seminal root and defective gravitropism. Seminal root elongation in the *our1* mutant was accelerated via the promotion of cell division and elongation. In addition, compared with the wild type, the density of short and thin lateral roots (S-type LRs) was reduced in the *our1* mutant, whereas that of long and thick LRs (L-type LRs) was increased. Expression of *OUR1*, which encodes OsbZIP1, a member of the basic leucine zipper transcription factor family, was observed in the seminal root tip and sites of LR emergence, wherein attenuation of reporter gene expression levels controlled by the auxin response promoter *DR5* was also observed in the *our1* mutant. Taken together, our results indicate that the *our1* gene promotes root development by suppressing auxin signaling, which may be a key factor contributing to an improvement in root architecture.

Keywords: auxin signaling, bZIP transcription factor, root development, root system architecture, mutant, rice

1. Introduction

A well-developed root system is important for the effective acquisition of water from soil, particularly in environments characterized by water deficits. The root system of rice is composed of the main roots, seminal root and crown roots, and their associated lateral roots (LRs). Due to the determination of the size at which roots can come into contact with the soil, the length of the main roots is well recognized as an important trait for plant productivity under water deficit conditions [1]. LRs have been categorized into two types based on their length, diameter, and histological characteristics [2,3,4]. The S-type LRs are short, thin, and lack branches, whereas the L-type LRs are long, thick, and have a high degree of branching. Therefore, L-type LRs can contribute to extending the entire root system to enhance water uptake and improve productivity, particularly with respect to shoot dry matter production and yield, via adaptation to stressful environments [5,6,7].

Evidence obtained from many studies, notably those on *Arabidopsis*, has highlighted the central role of auxins in orchestrating final root architecture and development via their coordination of molecular responses [8]. Studies on rice have also indicated the importance of auxin in root development. For example, the exogenous application of auxin results in inhibited elongation of seminal and crown roots [9,10,11], whereas it enhances the formation of both LRs and crown roots [12,13,14]. Consequently, under conditions of excess auxin synthesis through overexpression of *YUCCA1*, an enzyme mediating auxin biosynthesis, root elongation was observed to be severely inhibited, whereas the formation of crown roots was promoted [15]. Furthermore, a number of auxin-

related mutants have been isolated from rice, among which, the mutant of *CRL4/OsGNOM1* impairs auxin transport in roots, resulting in auxin-related abnormal phenotypes, such as reduced LR numbers and impaired root gravitropism [16,17]. Similarly, a rice gain-of-function mutant of *OsIAA13* has been shown to be associated with defective LR initiation, root hair formation, and gravitropism, attributable to stabilization of the OsIAA13 protein, which prevents auxin signal transduction [18]. A further gain-of-function mutant in *OsIAA11* has been observed to be associated with the inhibition of LR development and promotion of seminal and crown root elongation in rice [19]. Moreover, the mutations of *CRL1/ARL1* and *CRL5*, which function downstream of auxin signaling pathways, have been found to play roles in the inhibition of crown root initiation [20]. However, most of these mutations have been found to have negative effects on root growth, such as repressing the initiation and development of root components. Therefore, despite the notable importance of well-developed root systems in plant productivity and adaptation to stress, the associated mechanisms and genetic determinants remain largely unknown, thus limiting their application as breeding indices.

In this study, we isolated a novel rice mutant, *outstanding rooting 1* (*our1*), which displayed developed root phenotypes, including elongated seminal root and increased numbers of L-type LRs. On the basis of the observations reported herein, we propose that OUR1, a member of the basic leucine zipper (bZIP) transcription factor family, regulates root development through auxin signaling.

2. Materials and Methods

2.1. Plant materials, growth conditions, and morphological characterization

The *our1* mutant was obtained by mutagenizing *Oryza sativa* cv. Kimmaze using *N*-methyl-*N*-nitrosourea (MNU), as previously described [21]. The seeds of wild-type (WT), *our1* mutant, and F_2 plants derived from crosses between the mutants and *Oryza sativa* cv. Kasalath were grown in tap water without nutrient supplementation in a growth chamber at 28°C under conditions of continuous illumination. Transgenic plants were grown in Murashige and Skoog (MS) medium [22] containing 3% (w/v) sucrose and 0.3% Gelrite.

For phenotypic characterization, seedlings of the *our1* mutant, its WT Kimmaze, *Osiaa13* [18] and its WT Taichung65 (*Oryza sativa* cv.) were grown for 2 weeks under the aforementioned growth conditions, and plant height and root phenotypic traits were measured. The lateral root initiation index (I_{LRI}) was calculated as described [23]. Root gravitropic responses were examined using 4-day-old seedlings. Eight hours after transfer to 1% agar plates, the roots were rotated from vertical to horizontal at 90° for 12 h.

2.2. Map-based cloning, plasmid constructs, and plant transformation

To map the causative gene of the *our1* mutant, we performed a linkage analysis using F_2 plants derived from a cross between the *our1* mutant and Kasalath. For complementation of the *our1* mutation and expression analysis of *OUR1* gene, the wild-type genomic sequence of 'Kimmaze' was amplified in the region extending from approximately −3 kbp to +0.8 kbp (considering the *OUR1* translation site

as +1 bp) and was cloned into the pGWB4 vector [24] to generate the *ProOUR1:OUR1-GFP* construct. A *DR5:NSL-3* × *Venus* construct was generated as reported previously [25]. The generated fusion constructs were introduced into the EHA105 strain of *Agrobacterium tumefaciens* via electroporation. Subsequently, the *ProOUR1:OUR1* and *ProOUR1:OUR1-GFP* constructs were transformed into the *our1* mutant, and the *DR5:NSL-3* × *Venus* construct was transformed into WT and *our1* mutant plants via *Agrobacterium*-mediated transformation, as described previously [26,27]. Transgenic plants were selected on MS medium containing 50 mg L^{-1} hygromycin at 30°C.

2.3. Histological analysis

Cell division in seminal root tip was observed using a Click-iT™EdU Alexa Fluor® Imaging Kit (Invitrogen/Molecular Probes). The roots of 4- and 11-day-old seedlings were exposed to 1 L of water supplemented with 0.0125 g EdU and 1 mL DMSO for 30 min, after which the root samples were prepared as described previously [25] for fluorescence observation using a laser scanning microscope (FV1000; Olympus).

To measure cell length, the seminal root of WT and *our1* mutant plants were fixed in FAA (formaldehyde: acetic acid:50% ethanol at 1:1:18) solution for 24 h and then dehydrated in a graded ethanol series. Subsequently, the samples were soaked in salicylic acid for transparency and observed under a laser scanning microscope (FV1000; Olympus).

2.4. Measurement of auxin levels

The content of endogenous indole acetic acid (IAA) was determined using a modified version of the method described by Kakiuchi [28] as follows. Approximately 100 mg of fresh seminal roots were collected from 4-day-old seedlings and ground in liquid nitrogen. Thereafter, 350 µL of 1.6×10^{-6} M indole-3-acetic-2,2-d2 acid (C/D/N Isotopes, Canada) in methanol was added to the samples as an internal standard to monitor IAA. The tubes were centrifuged at 20,000 × *g* and 250 µL of the resulting supernatants was pre-purified by passing through a reverse-phase column (C18 Sep-Pak; Waters, Japan). Sample volumes were made up to 1000 µL with distilled water, and the pH was adjusted to 2.8 with 2 M phosphoric acid. The samples were then extracted four times with an equal volume of diethyl ether, and following the evaporation of ether, the samples were dissolved in 50 µL 85% (v/v) methanol. Aliquots (10 µL) of the samples were analyzed using a liquid chromatography–tandem mass spectrometry system (HPLC: Ultimate 3000; Thermo Fisher Scientific, USA) equipped with a 5-µm Hypersil GOLD column (50 mm × 2.1 mm; Thermo Fisher Scientific). Data are expressed as the average of three biological replications.

2.5. Expression analysis

Total RNA was extracted from the seminal root of WT and *our1* mutant seedlings using a NucleoSpin RNA Plant Kit (Macherey-Nagel) according to the manufacturer's instructions. Quantitative real-time PCR (qRT-PCR) was performed using a One-Step SYBR PrimeScript RT-PCR

Kit II (Perfect Real Time; TaKaRa Bio) and StepOnePlus Real-Time PCR (Life Technologies). The expression levels of each gene were normalized to the expression level of ubiquitin, which was used as an internal control. The seminal root was further segmented to different zones representing the different LR developmental stages as shown in Supplementary Fig. 2 for expression analysis of *OUR1/OsbZIP1*. The primer sequences used for qRT-PCR are listed in Supplementary Table 2.

To observe the GFP expression of *ProOUR1:OUR1-GFP* in *our1* mutant roots, transgenic plants were embedded in 5% agar medium and the seminal root and LRs were sectioned into 100-μm-thick sections using a vibrating blade microtome (Leica). Images were captured using a laser scanning microscope (FV1000; Olympus).

For observations of the expression of *DR5:NLS-3 × Venus* in WT and *our1* mutant plants, 2-cm sections from the tips of seminal root and sites of LR emergence were sampled and viewed under a laser scanning microscope (FV1000; Olympus).

2.6. Statistical analysis

The inheritance mode of *our1* mutant phenotypic traits was examined by determining the segregation ratio of the phenotype in each M_3 progeny using the Chi-square test. The shoot and root characteristics, expression levels of *OUR1* and other genes in the roots, copy number of the reporter gene in transgenic plants, and IAA contents were compared using a Student's *t*-test or analysis of variance (ANOVA) followed by a multiple-comparison Tukey test in R commander version 3.5.1. [29].

3. Results

3.1. Phenotypic characterization of the *our1* mutant

To gain an understanding of the molecular mechanisms underlying the regulation of root system development, we screened a rice mutant line with promoted root growth (Fig. 1A). Compared with the WT, the *our1* mutant was characterized by approximately three-fold longer seminal root and a lower number of crown roots, whereas plant heights were comparable (Fig. 1B-D). Although the total number of LRs per seminal root in the *our1* mutant was higher than that in the WT, owing to the longer seminal root length in the *our1* mutant, the density of total LRs was significantly reduced (Fig. 1E, F). Interestingly, however, despite the lower density of total and S-type LRs, the density of L-type LRs was observed to be significantly higher in the *our1* mutant (Fig. 1G, H). The I_{LRI} of all lateral root components, that is total, S-type, and L-type lateral roots, were consistent with those of the lateral root density, additionally supporting that the initiation ability of total and S-type LRs were suppressed but that of the L-type was promoted in the *our1* mutant (Supplementary Table 1). Because the *Osiaa13* mutant, which characterized in our previous study to be defective in auxin signal transduction [18], showed similar root phonotypes with that of the *our1* mutant, the comparison of these two mutants allowed us to concentrate on auxin signaling initially in control of root development in the *our1* mutant. In fact, the root phenotypes in the *our1* mutant, which described above, were similar to those of the *Osiaa13* mutant in terms of promotion of seminal root elongation, a reduction in the density of total

and S-type LRs, and an increased density of L-type LRs (Fig. 1A, C, F, G, and H). These results indicate that the root phenotypes of the *our1* mutant could be regulated by auxin.

We therefore examined the gravitropic response of roots, a typical auxin-related phenotype [13,16,18,20], and accordingly found that whereas WT roots showed a pronounced response to changes in the gravity vector, the response of *our1* mutant roots was impaired. All WT roots had root tip angles of 60°–90°, whereas the root tip angles of the *our1* mutant showed a wider range of distribution from 40° to 90°, resulting in significantly lower root tip angles in the *our1* mutant compared to the WT (Fig. 1I-K, Supplementary Table 1). Impaired root gravitropism has similarly been observed in the *Osiaa13* mutant [18], and thus we assumed the auxin response system in the *our1* mutant to be defective.

3.2. Auxin responses are inhibited in the mutant

To investigate the auxin response in *our1* mutant roots, we analyzed the expression patterns of early auxin response genes, *Aux/IAAs*. Among the 31 *Aux/IAA* members in rice, 19 *Aux/IAA* genes were selected based on their expression pattern, which was relatively higher in the roots [30,31]. In most cases, the expression of these genes was significantly lower in the *our1* mutant than in the WT, among which, the expression of *OsIAA20* and *OsIAA24*, which show a pronounced response to exogenous auxin treatment in roots [30,31], was severely repressed in *our1* mutant plants (Fig. 2A). On the other hand, the expression of *OsIAA13*, which show a weak response to exogenous auxin treatment in roots [30,31], did not differ between the *our1* mutant and the WT (Fig. 2A). In contrast, the auxin content in the *our1* mutant roots was observed to be comparable to that in WT roots (Fig. 2B). These findings thus tend to indicate that auxin signaling is suppressed in roots of the *our1* mutant.

While several phytohormones are involved in regulating root development, cytokinin is known to be another major player for both crown and lateral roots formation by acting antagonistically to auxin [20, 32, 33]. The expression of a cytokinin oxidase/dehydrogenase (CKX) family gene, *OsCKX4*, and a cytokinin response regulator, *OsRR2*, which are known to be related to cytokinin signaling mediated root formation [32], did not differ in the *our1* mutant root and the WT root (Supplementary Fig. 1). This result further supports our findings that the decreased lateral root density in the *our1* mutant may be caused by auxin but not by cytokinin.

3.3. Isolation of the causative gene of the *our1* mutant and its expression patterns in roots

To map the causative gene, an F_2 population was generated by crossing the *our1* mutant (derived from Kimmaze, a *japonica* variety) with WT Kasalath (an *indica* variety). Seedlings display a well-developed root system among the progeny segregated in a 3:1 WT:mutant ratio, indicating that the mutant phenotype is caused by a single recessive gene. Using these seedlings, we employed a map-based cloning approach to isolate the causal gene, and accordingly identified a locus on chromosome 1, located in an approximately 113-kb region between the molecular markers KW02 and KW04 (Fig. 3A). Within this region, we detected a single nucleotide substitution from C to T, which resulted in a

single amino acid substitution from glutamic acid to a stop codon, in the second exon of an ORF, Os01g0174000 (Fig. 3A).

First, the expression pattern of this *OUR1* candidate gene at different LR developmental stages was compared between the WT and the *our1* mutant. In all zones, the expression of the candidate gene was significantly lower in the *our1* mutant than in the WT, among which, the expressions in the LR primordium induction zones were highest in the WT but greatly reduced in the mutant (Supplementary Fig. 2). Therefore, we checked approximately -3 kb promoter region of the candidate gene and found that there was no difference on the sequence between the mutant and the WT. Then, we introduced the WT *OUR1* candidate gene under the control of its promoter (*proOUR1:OUR1*) into the *our1* mutant. The resultant transgenic plants were found to lack a developed root phenotype, whereas regenerated *our1* mutant plants without the *proOUR1:OUR1* construct were characterized by well-developed roots (Fig. 3B), and we accordingly concluded that the root phenotype of the *our1* mutant is caused by a mutation in *OUR1* gene (Os01g0174000).

The *OUR1* gene encodes OsbZIP1, a member of the bZIP transcription factor family, which is a rice homolog of the *Arabidopsis* Elongated Hypocotyl5 (HY5) transcription factor [34]. The OUR1/OsbZIP1 protein contains a conserved interaction motif at amino acids 43 to 54, which interacts with Constitutive Photomorphogenic Protein 1 (COP1) and a bZIP domain at amino acids 110 to 166, and the site of the *our1* mutation is located at amino acid 79 (Fig. 3A). We assume that the mutation disrupts the function of the bZIP domain, giving rise to the loss-of-function of OUR1/OsbZIP1 protein.

We examined the expression pattern of *OUR1/OsbZIP1* in *our1* mutant roots using GFP fluorescence controlled by the *OUR1* promoter, and accordingly detected GFP fluorescence in regions of the seminal root tip, including the root apical meristem (RAM), root cap, and elongation zone (Fig. 3C). To observe this distribution more clearly, we prepared cross-sections from the tip of the RAM (Fig. 3F), the basal part of the RAM (Fig. 3E), and the elongation zone (Fig. 3D), and observed GFP fluorescence in whole tissues. Furthermore, we observed cross-section prepared from the site of LR emergence, and found strong expression in the RAM and elongation zone of the LRs (Fig. 3G). In contrast, we detected autofluorescence but no GFP fluorescence in the seminal root tips and cross-sections of transformants carrying the *ProOUR1:OUR1* construct, which we used as a negative control (Fig. 3H, I).

3.4. The *our1* mutation promotes root elongation by enhancing cell division and elongation

Given that expression of *OUR1/OsbZIP1* was observed in both the division zone and elongation zone in seminal root tip (Fig. 3), we compared cell division and elongation in *our1* mutant and WT plants (Fig. 4). Cell division was visualized by applying EdU to the RAM of the seminal root. At the early seedling stage (4 day after sowing, DAS), the *our1* mutant showed a higher rate of cell division compared with the WT (Fig. 4A). We thus compared RAM size in *our1* mutant and WT seedlings, determined according to the length from the lowermost to the uppermost dividing cells, and found that the *our1* mutant had a wider zone of division compared with the WT (Fig. 4C). At the late

seedling stage (11 DAS), we detected a marked attenuation of the EdU signal in WT plants, whereas the signal was still maintained to a certain extent in the *our1* mutant (Fig. 4B, C). Subsequently, we compared cell lengths in the mature zone and observed that the length of cells in the *our1* mutant was longer than that in the WT (Fig. 4D). Moreover, the length of cortex cells in the *our1* mutant was approximately two times that in the WT (Fig. 4E). Although the root diameter in the mature zone did not differ between the genotypes, the cell area in the *our1* mutant was significantly higher than that of the WT, resulting from the difference in the cell length (Supplementary Table 1). These observations thus indicate that the *our1* mutation promotes root growth via a prolonged and higher rate of cell division and greater cell elongation.

3.5. OUR1/OsbZIP1 positively regulates auxin signaling

The expression pattern of *NLS-3* × *Venus* driven by the auxin response promoter *DR5* (*DR5:NLS-3* × *Venus*) was analyzed in the seminal root tip and LR emergence site, wherein the expression of *OUR1/OzbZIP1* had been observed (Fig. 5). In the WT, we observed normal auxin signals, with strong signals in the center of the root cap, quiescent center (QC), and the vascular bundles (Fig. 5A-C). In *our1* mutant, however, the signals were comparatively weak and confined to the center of the root cap and QC, whereas no signals were detected in the vascular bundles (Fig. 5D-F). Furthermore, at the site of LR emergence in WT seedlings we detected strong signals at the center of the lateral root primordium (LRP) (Fig. 5G-I), whereas few signals were detected in the *our1* mutant (Fig. 5J-L). To examine the visualized auxin signals quantitatively, we performed qRT-PCR using T_1 plants of the WT and *our1* mutant, having previously determined segregation of the copy number of the *DR5:NLS-3* × *Venus* T-DNA region in the genomic DNA of the T_1 plants. This preliminary assessment revealed that #WT-2, and #*our1*-1 had no T-DNA copies. On the other hand, the copy numbers in #WT-5, #WT-6, #*our1*-5, and #*our1*-6 were almost twice as high as those in #WT-3, #WT-4, #*our1*-2, #*our1*-3, #*our1*-4, and #WT-1, indicating that the former have two T-DNA copies and the latter have one copy (Fig. 5M). Using the former plants, we compared the relative *Venus* expression levels and found that these were significantly lower in the *our1* mutant than in the WT (Fig. 5N), thereby indicating that OUR1/OsbZIP1 positively regulates auxin signaling.

3.6. OUR1/OsbZIP1 might control root phenotype through regulating auxin-related genes

As mentioned above, we assume that the longer seminal root of the *our1* mutant is attributable to a promotion of cell elongation. To investigate the effect of the *our1* mutation on the expression of genes related to cell elongation, we selected α-Expansin genes that encode cell wall loosening proteins, the activity of which can promote cell elongation [35,36]. Among these genes, we analyzed the expression patterns of *OsEXPA18* and *OsEXPA28*, which revealed high expression in rice roots and auxin responsive based on a RiceXPro database (https://ricexpro.dna.affrc.go.jp). We initially confirmed the response to exogenous auxin treatment in the WT, which revealed the repression of the expression of both *OsEXPA18* and *OsEXPA28* (Fig. 6A). Subsequently, we examined the expressions

of these genes in the *our1* mutant and WT and found that the expression of both *OsEXPA18* and *OsEXPA28* was significantly higher in the *our1* mutant than in the WT (Fig. 6C).

Given that our phenotypic characterization had revealed that the density of total LRs was significantly lower in the *our1* mutant than in the WT, we analyzed the expression of genes involved in the regulation of LR development in *our1* mutant and WT plants. In this regard, previous studies have indicated that LR initiation and development in rice and *Arabidopsis* are controlled by lateral organ boundary-domain (LBD) genes [13,37]. Among these genes, we selected and analyzed the expression pattern of *CRL1/ARL1* and *OsLBD2-1/DH1*, which are homologous to *Arabidopsis* LBD16 and LBD29, which are essential genes for LR development [13,37,38,39]. We accordingly observed that the expression of *CRL1/ARL1* and *OsLBD2-1/DH1* was significant induced by exogenous auxin application in WT plants and showed comparatively significantly inhibition in the *our1* mutant (Fig. 6B, D). Similarly, the genes repressed by auxin in the WT were induced in the *our1* mutant, whereas the genes that were promoted by auxin in the WT were repressed in the *our1* mutant. These observations thus indicate that the altered expression of these auxin-responsive genes via repression of auxin signaling in the *our1* mutant leads to an increase in seminal root length and a reduction in total LR density.

4. Discussions

In this study, we report a new rice mutant line, *our1*, which is characterized by a well-developed root system. The altered root phenotypes observed in *our1* mutants, including elongated seminal root and lower total LR density, are typical auxin-related phenotypes in both rice and *Arabidopsis* [8,16,18,19]. Defective gravitropism, diminished auxin signaling, phenotypic traits similar to those of the *Osiaa13* mutant, and the repressed expression of auxin-inducible genes, collectively provide compelling evidence that the root phenotypes of the *our1* mutant are controlled by auxin signaling (Fig. 1, 2, 5, and 6).

4.1. *our1* mutation might enhance root elongation through restricting auxin signaling

Root growth is primarily regulated by two coordinated processes, namely, cell division and expansion [40]. We found that the seminal root of the *our1* mutant were approximately three times longer than those of the WT. Expression of the causal gene of the *our1* mutant was observed in both the division zone and elongation zone in seminal root tips, indicating that root elongation in the *our1* mutant is attributable to the regulation of both cell division and elongation (Fig. 3C-F). Root length is correlated with the size of root meristems and the number of meristematic cells [11,41], and the more prolonged and higher rate of cell division over a wider region in the *our1* mutant compared with the WT is assumed to promote elongation of the seminal root (Fig. 4A-C). Furthermore, the length of cells in the mature zone of *our1* mutant roots was found to be significantly longer than that in WT roots, thereby indicating that the elongated length of individual cells in the *our1* mutant also accelerated the elongation of seminal root length (Fig. 4D, E). Expansin genes are known to be involved in cell

elongation by mediating cell wall loosening [35,36,42], and numerous studies on rice have reported that knockdown of Expansins leads to a reduction in both individual cell length and overall root length [36,43]. In the present study, we observed that the expression of *OsEXPA18* and *OsEXP28* was significantly higher in the *our1* mutant than in the WT, indicating that OUR1/OsbZIP1 inhibits root growth by repressing the expression of these two genes (Fig. 6C). Furthermore, the expression of *OsEXPA18* and *OsEXP28* was shown to suppressed by exogenous auxin treatment (Fig. 6A). These results thus propose that OUR1/OsbZIP1 represses the expression of *OsEXPA18* and *OsEXP28* by promoting auxin signaling, resulting in a negative regulation of the elongation of individual cells and whole seminal root.

4.2. *OUR1/OsbZIP1* might control crown root and LR formation through the regulation of auxin signaling

Reductions in crown root and LR formation are typical auxin-related phenotypes observed in certain rice mutants. Stabilized IAA proteins in rice gain-of-function mutants of *OsIAA11, OsIAA13*, and *OsIAA23* have been shown to be associated with the impaired initiation of crown roots and/or LRs [18,19,44]. Similar to the *our1* mutant, the mutations in auxin-inducible genes that function downstream of auxin signaling, *CRL1/ARL1*, *CRL4*/*OsGNOM1*, and *CRL5*, have been found to inhibit the initiation of crown roots and/or LRs [13,16,20]. In the *our1* mutant, the expression of *CRL1/ARL1* and *OsLBD2-1/DH1*, which are known to be involved in the initiation and development of lateral organ primordia, was significantly repressed compared with that in the WT (Fig. 6D). These results thus indicate that OUR1/OsbZIP1 promotes the expression of *CRL1/ARL1* and *OsLBD2-1/DH1* via the promotion of auxin signaling, resulting in a positive regulation of the initiation of crown roots and LRs. The insignificant difference in the change of crown root number in the *Osiaa13* mutant, and the significant reduction in the *our1* mutant (Fig. 1D, E) can be attributed to the variations and redundancies of 31 *Aux/IAA* members, such as rare activation of *OsIAA13* functions in crown root initiation [18]. It has been also reported that auxin signaling was not restricted at the crown root initiation sites in the *Osiaa13* mutant [18]. On the other hand, in the *our1* mutant, the crown root initiation may be reduced by the restricted auxin signaling.

Regarding a parameter for LR initiation, I_{LRI} is a useful parameter to accurately understand the LR initiation ability [23] particularly in cases where the individual cell length differed such as in the *our1* mutant. The significantly increased total LR number in the *our1* mutant can be attributed to the approximately three times longer seminal root length in the mutant than the WT which resulted in significantly low LR density and I_{LRI} (Fig. 1, Supplementary Table 1). The I_{LRI} was consistent with the lateral root density in terms of all lateral root components, that is total, S-type, and L-type LRs. This further supports our findings that the total lateral root initiation ability is suppressed in the *our1* mutant.

Interestingly, although total LR density in the *our1* mutant was significantly lower than that in the WT, the *our1* mutant showed a reduction only in the density of S-type LRs whereas an increase in the density of L-type LRs (Fig. 1). The *Osiaa13* mutant, which is characterized by defects in auxin

signal transduction, shows the same tendency (Fig. 1), indicating that a reduction in auxin signaling play an important role in inducing L-type LR formation subsequent to initiation.

4.3. OUR1/OsbZIP1, a homolog of *Arabidopsis* HY5, controls root phenotypes

The causal gene isolated from the *our1* mutant encodes OsbZIP1, a member of the bZIP transcription factor family, which is known as a rice homolog of the *Arabidopsis* HY5 transcription factor [34]. In *Arabidopsis*, HY5 has been characterized as a positive regulator of photomorphogenesis [45], which functions as an integrator of light, hormone, and stress signaling [46]. A number of studies on *hy5* mutants have revealed that HY5 also controls root growth, as the *hy5* mutant exhibits increased LR density and defective gravitropism, which are recognized auxin-related phenotypes [45,47,48]. HY5 is strongly expressed in the LRPs, wherein higher auxin signaling has been observed in the *hy5* mutant compared with the corresponding WT [49]. Thus, it has been established that HY5 negatively regulates auxin signaling, resulting in a decrease of LR density [47,48]. However, the increased auxin signaling observed in the *hy5* mutant contrasts with the reduction in auxin signaling seen in the *our1* mutant (Fig. 5). In this regard, phylogenetic analysis has indicated that there are three rice bZIP transcript factors (OsbZIP1, OsbZIP18, and OsbZIP48) that are closely related to HY5 [50], among which, OsbZIP48 has been shown to be a functional ortholog of HY5, given that it is able to complement the *hy5* mutant with respect to hypocotyl elongation growth in the light [34]. Considering that a functional difference between OsbZIP18 and OsbZIP48 has also been reported [50], we suspect that there might be differences between these genes and OsbZIP1 with respect specific and/or redundant functions. Consequently, further analysis of these genes is needed to confirm their differentiated functional roles in the growth and development of rice.

5. Conclusions

In this study, we isolated the *our1* mutant, which is characterized an increase in main root length and L-type lateral roots. We speculate that mutation of the *OUR1/OsbZIP1* gene might control root architecture by reducing auxin signaling and altering the expression of auxin-responsive genes, such as *OsEXPAs* and *OsLBDs*. Although a number of previous studies have reported the importance of a larger root system, including an increase in main root length and L-type lateral roots, for water absorption, which contribute to shoot dry matter production and yield under water deficit conditions, the information on useful genes for such breeding purposes is still limited. In this regard, the mutation of *OUR1/OsbZIP1*, which leads to a well-developed root system without adverse effects on shoot growth and development, would be a key factor in developing a new breeding strategy designed to improve root architecture.

Acknowledgements

We thank Ms. Kimiyo Inukai, Ms. Eiko Murakami and Ms. Saki Nishiuchi for their valuable

technical support. This work was supported by the Japan Science and Technology Agency (JST)/Japan International Cooperation Agency (JICA) and the Science and Technology Research Partnership for Sustainable Development (SATREPS, No. JPMJSA1706), JSPS KAKENHI Grant Number 18H02174, and 19J13009.

Figure legends

Fig. 1. Phenotypes of the *our1* and *Osiaa13* mutants. (A) Two-week-old seedlings grown in tap water under continuous light conditions. SR, seminal root; CR, crown root; LR, lateral root. Scale bar = 5 cm. (B-H) Shoot and root traits measured at 2 weeks after sowing. Values represent the means ± SE (n = 10). (I-K) The gravitropic responses of seminal root tip. Root tip angles induced by gravistimulation (θ) (I), its response in a seminal root of the wild type (WT) (above) and the *our1* mutant (bellow) (J), and its distribution (K). Arrowheads indicate the point of rotation from vertical to horizontal at 90°. Scale bar = 2 cm. Statistical significance at ns (not significant), $*P < 0.05$ and $**P < 0.01$ between genotypes was determined using Student's *t*-test.

Fig. 2. Expression of *Aux/IAA* genes and auxin concentrations. (A) Changes in the expression levels of 19 *OsIAA* genes. Horizontal bars indicate the expression level of the *our1* mutant relative to that of the wild type (WT), considering expression level in the WT to be 1. (B) Auxin concentrations in whole seminal root of 4-day-old WT and *our1* mutant. Values represent means ± SE (n = 3). Statistical significance at ns (not significant), $*P < 0.05$ and $**P < 0.01$ between genotypes was determined using Student's *t*-test.

Fig. 3. Gene isolation, complementation test, and expression pattern of the *OUR1* gene. (A) High-resolution linkage and physical map of the *OUR1* locus and the structure of the *OUR1* gene on chromosome 1. Black boxes and horizontal lines indicate the exons and introns, respectively. The arrowhead indicates a C/T single nucleotide substitution at base pair 332 in the second exon that resulted in a single amino acid substitution from glutamic acid to a stop codon. Regions I and II indicate a motif related to interaction with COP1 and a bZIP domain, respectively. (B) Complementation test of the *OUR1* gene. From left to light, regenerated plants of the *our1* mutant harboring the *proOUR1: OUR1* construct, wild-type (WT) plant, the *our1* mutant, and the vector control. Scale bar = 5 cm. (C-G) Expression patterns of the *OUR1* gene in seminal root tip in vertical (C), and horizontal section through the elongation zone (D) and in the basal part of the root apical meristem (RAM) (E), the tip of the RAM (F), and the site of lateral root emergence (G). (H, I) Expression pattern of negative control in seminal root tip vertical (H) and horizontal (I) sections. Scale bars = 50 μm.

Fig. 4. Comparison of the cell division and cell elongation in wild-type (WT) and *our1* mutant roots. (A-C) Dividing cells in the root apical meristem (RAM), represented by green color, of 4-day-old (A) and 11-day-old (B) WT and *our1* mutant seedlings, and a comparison of RAM size (C). The

size of the RAM is determined by the length from the lowermost to the uppermost dividing cells, as indicated by the arrowheads. (D, E) Mature cortex cells in the elongation zone of the WT and *our1* mutant seedlings (D), and the corresponding cell lengths (E). Scale bars = 50 μm. Values represent the means ± SE (n = 3). Statistical significance at ns (not significant) and $^{**}P < 0.01$ between genotypes was determined using Student's *t*-test.

Fig. 5. Auxin distribution pattern and expression analysis. (A-L) Auxin distribution pattern represented by the expression of *DR5:NLS-3* × *Venus* in seminal root tip in wild-type (WT) (A-C) and *our1* mutant (D-F) seedlings, and at the site of lateral root emergence in WT (G-I) and *our1* mutant (J-L) seedlings. Scale bars = 100 μm. (M, N) Relative copy number of *NLS-3* × *Venus* (M) and its expressions with a double copy of *NLS-3* × *Venus* (N). Different letters indicate significant differences between groups ($P < 0.05$, one-way ANOVA followed by Tukey's test for multiple comparisons); Values represent the means ± SE (n = 3).

Fig. 6. Expression of auxin-related genes. (A, B) Expressions of the *OsEXPA* (A) and *OsLBD* (B) genes with/without exogenous indole acetic acid (IAA: 1 mM) treatment for 1 h. (C, D) Expression of the *OsEXPA* (A) and *OsLBD* (B) genes in wild-type (WT) (C) and *our1* mutant (D) seedlings. Values represent the means ± SE (n = 3). Statistical significance at ns (not significant) and $^{**}P < 0.01$ between treatments or genotypes was determined using Student's *t*-test.

Supplementary Fig. 1. Expression of cytokinin-related genes. (A, B) Expressions of the *OsCKX4* (A) and *OsRR2* (B) genes in wild-type (WT) and *our1* mutant. Values represent the means ± SE (n = 3). ns, not significant by Student's *t*-test.

Supplementary Fig. 2. Expression patterns of *OUR1/OsbZIP1* at different zone of the seminal root. Seminal root at 5 days after sowing is divided into following four zones: Zone 1, approximately 5 mm from the root tip; Zone 2, induction of LR primordium; Zone 3, formation of LR primordium; Zone 4, Emerged LRs. LR, lateral root. Different letters indicate significant differences between genotypes across root zones ($P < 0.05$, one-way ANOVA followed by Tukey's test); Values represent the means ± SE (n = 3).

Supplementary Table 1. Comparison of root traits between the WT and *our1* mutant. Values represent means ± SE (n = 10). $^{*}P < 0.05$, $^{**}P < 0.01$, and ns, not significant by Student's *t*-test. LR, lateral root.

Supplementary Table 2. List of primers used for qRT-PCR

References

[1] E. Kameoka, R.R. Suralta, S. Mitsuya, A. Yamauchi, Developmental plasticity of rice root system grown under mild drought stress condition with shallow soil depth; Comparison between nodal and lateral roots, Plant Prod. Sci. 19 (2016) 411–419. https://doi.org/10.1080/1343943X.2015.1128094.

[2] Y. Kono, M. Igeta, N. Yamada, Studies on the developmental physiology of the lateral roots in rice seminal roots, Proc. Crop Sci. Soc. Japan 41 (1972) 192–204.

[3] A. Yamauchi, Y. Kono, J. Tatsumi, Quantitative analysis on root system structures of upland rice and maize, Jpn. J. Crop Sci. 56 (1987) 608–617.

[4] T. Kawai, M. Nosaka-Takahashi, A. Yamauchi, Y. Inukai, Compensatory growth of lateral roots responding to excision of seminal root tip in rice, Plant Root. 11 (2017) 48–57. https://doi.org/10.3117/plantroot.11.48.

[5] J.M. Niones, R.R. Suralta, Y. Inukai, A. Yamauchi, Field evaluation on functional roles of root plastic responses on dry matter production and grain yield of rice under cycles of transient soil moisture stresses using chromosome segment substitution lines, Plant Soil. 359 (2012) 107–120. https://doi.org/10.1007/s11104-012-1178-7.

[6] M. Kano-Nakata, V.R.P. Gowda, A. Henry, R. Serraj, Y. Inukai, D. Fujita, N. Kobayashi, R.R. Suralta, A. Yamauchi, Field Crops Research. Functional roles of the plasticity of root system development in biomass production and water uptake under rainfed lowland conditions, 144 (2013) 288–296.

[7] R.R. Suralta, M. Kano-Nakata, J.M. Niones, Y. Inukai, E. Kameoka, T.T. Tran, D. Menge, S. Mitsuya, A. Yamauchi, Root plasticity for maintenance of productivity under abiotic stressed soil environments in rice: Progress and prospects, F. Crop. Res. 220 (2018) 57–66. https://doi.org/10.1016/j.fcr.2016.06.023.

[8] P. Overvoorde, H. Fukaki, T. Beeckman, Auxin control of root development., Cold Spring Harb. Perspect. Biol. 2 (2010) 1–17. https://doi.org/10.1101/cshperspect.a001537.

[9] L. Eliasson, G. Bertell, E. Bolander, Inhibitory Action of Auxin on Root Elongation Not Mediated by Ethylene, Plant Physiol. 91 (1989) 310–314. https://doi.org/10.1104/pp.91.1.310.

[10] Y. Song, Z.F. Xu, Ectopic overexpression of an AUXIN/INDOLE-3-ACETIC ACID (Aux/IAA) gene OsIAA4 in rice induces morphological changes and reduces responsiveness to auxin, Int. J. Mol. Sci. 14 (2013) 13645–13656. https://doi.org/10.3390/ijms140713645.

[11] C. Yu, C. Sun, C. Shen, S. Wang, F. Liu, Y. Liu, Y. Chen, C. Li, Q. Qian, B. Aryal, M. Geisler, D.A. Jiang, Y. Qi, The auxin transporter, OsAUX1, is involved in primary root and root hair elongation and in Cd stress responses in rice (Oryza sativa L.), Plant J. 83 (2015) 818–830. https://doi.org/10.1111/tpj.12929.

[12] T. Chhun, S. Taketa, S. Tsurumi, M. Ichii, The effects of auxin on lateral root initiation and root gravitropism in a lateral rootless mutant Lrt1 of rice (Oryza sativa L.), Plant Growth Regul. 39 (2003) 161–170. https://doi.org/10.1023/A:1022592511387.

[13] Y. Inukai, T. Sakamoto, M. Ueguchi-Tanaka, Y. Shibata, K. Gomi, I. Umemura, Y. Hasegawa, M. Ashikari, H. Kitano, M. Matsuoka, Crown rootless1, which is essential for crown root formation in rice, is a target of an Auxin Response Factor in auxin signaling, Plant Cell. 17 (2005) 1387–1396. https://doi.org/10.1105/tpc.105.030981.

[14] M. Xu, L. Zhu, H. Shou, P. Wu, A PIN1 family gene, OsPIN1, involved in auxin-dependent adventitious root emergence and tillering in rice, Plant Cell Physiol. 46 (2005) 1674–1681. https://doi.org/10.1093/pcp/pci183.

[15] Y. Yamamoto, N. Kamiya, Y. Morinaka, M. Matsuoka, T. Sazuka, Auxin biosynthesis by the YUCCA genes in rice, Plant Physiol. 143 (2007) 1362–1371. https://doi.org/10.1104/pp.106.091561.

[16] Y. Kitomi, A. Ogawa, H. Kitano, Y. Inukai, CRL4 regulates crown root formation through auxin transport in rice, Plant Root. 2 (2008) 19–28. https://doi.org/10.3117/plantroot.2.19.

[17] S. Liu, J. Wang, L. Wang, X. Wang, Y. Xue, P. Wu, H. Shou, Adventitious root formation in rice requires OsGNOM1 and is mediated by the OsPINs family, Cell Res. 19 (2009) 1110–1119. https://doi.org/10.1038/cr.2009.70.

[18] Y. Kitomi, H. Inahashi, H. Takehisa, Y. Sato, Y. Inukai, OsIAA13-mediated auxin signaling is involved in lateral root initiation in rice, Plant Sci. 190 (2012) 116–122. https://doi.org/10.1016/j.plantsci.2012.04.005.

[19] Z.X. Zhu, Y. Liu, S.J. Liu, C.Z. Mao, Y.R. Wu, P. Wu, A gain-of-function mutation in OsIAA11 affects lateral root development in rice, Mol. Plant. 5 (2012) 154–161. https://doi.org/10.1093/mp/ssr074.

[20] Y. Kitomi, H. Ito, T. Hobo, K. Aya, H. Kitano, Y. Inukai, The auxin responsive AP2/ERF transcription factor CROWN ROOTLESS5 is involved in crown root initiation in rice through

the induction of OsRR1, a type-A response regulator of cytokinin signaling, Plant J. 67 (2011) 472–484. https://doi.org/10.1111/j.1365-313X.2011.04610.x.

[21] H. Inahashi, I.J. Shelley, T. Yamauchi, S. Nishiuchi, M. Takahashi-Nosaka, M. Matsunami, A. Ogawa, Y. Noda, Y. Inukai, OsPIN2, which encodes a member of the auxin efflux carrier proteins, is involved in root elongation growth and lateral root formation patterns via the regulation of auxin distribution in rice, Physiol. Plant. 164 (2018) 216–225. https://doi.org/10.1111/ppl.12707.

[22] T. Murashige, F. Skoog, A Revised Medium for Rapid Growth and Bio Assays with Tobacco Tissue Cultures, Physiol. Plant. 15 (1962) 473–497. https://doi.org/10.1111/j.1399-3054.1962.tb08052.x.

[23] J.G. Dubrovsky, A. Soukup, S. Napsucialy-Mendivil, Z. Jeknić, M.G. Ivanchenko, The lateral root initiation index: An integrative measure of primordium formation, Ann. Bot. 103 (2009) 807–817. https://doi.org/10.1093/aob/mcn267.

[24] T. Nakagawa, T. Suzuki, S. Murata, S. Nakamura, T. Hino, K. Maeo, R. Tabata, T. Kawai, K. Tanaka, Y. Niwa, Y. Watanabe, K. Nakamura, T. Kimura, S. Ishiguro, Improved gateway binary vectors: High-performance vectors for creation of fusion constructs in transgenic analysis of plants, Biosci. Biotechnol. Biochem. 71 (2007) 2095–2100. https://doi.org/10.1271/bbb.70216.

[25] N. Lucob-Agustin, T. Kawai, M. Takahashi-Nosaka, M. Kano-Nakata, C.M. Wainaina, T. Hasegawa, M. Inari-Ikeda, M. Sato, H. Tsuji, A. Yamauchi, Y. Inukai, WEG1, which encodes a cell wall hydroxyproline-rich glycoprotein, is essential for parental root elongation controlling lateral root formation in rice, Physiol. Plant. 169 (2020) 214–227. https://doi.org/10.1111/ppl.13063.

[26] Y. Hiei, S. Ohta, T. Komari, T. Kumashiro, Efficient transformation of rice (Oryza sativa L.) mediated by Agrobacterium and sequence analysis of the boundaries of the T-DNA, Plant J. 6 (1994) 271–282. https://doi.org/10.1046/j.1365-313X.1994.6020271.x.

[27] K. Ozawa, Establishment of a high efficiency Agrobacterium-mediated transformation system of rice (Oryza sativa L.), Plant Sci. 176 (2009) 522–527. https://doi.org/10.1016/j.plantsci.2009.01.013.

[28] Y. Kakiuchi, I. Gàlis, S. Tamogami, H. Wabiko, Reduction of polar auxin transport in tobacco by the tumorigenic Agrobacterium tumefaciens AK-6b gene, Planta. 223 (2006) 237–247. https://doi.org/10.1007/s00425-005-0080-4.

[29] J. Fox, The R Commander: A basic-statistics graphical user interface to R, J. Stat. Softw. 14 (2005). https://doi.org/10.18637/jss.v014.i09.

[30] M. Jain, N. Kaur, R. Garg, J.K. Thakur, A.K. Tyagi, J.P. Khurana, Structure and expression analysis of early auxin-responsive Aux/IAA gene family in rice (Oryza sativa), Funct. Integr. Genomics. 6 (2006) 47–59. https://doi.org/10.1007/s10142-005-0005-0.

[31] H. Takehisa, Y. Sato, M. Igarashi, T. Abiko, B.A. Antonio, K. Kamatsuki, H. Minami, N. Namiki, Y. Inukai, M. Nakazono, Y. Nagamura, Genome-wide transcriptome dissection of the rice root system: Implications for developmental and physiological functions, Plant J. 69 (2012) 126–140. https://doi.org/10.1111/j.1365-313X.2011.04777.x.

[32] S. Gao, J. Fang, F. Xu, W. Wang, X. Sun, J. Chu, B. Cai, Y. Feng, C. Chu, CYTOKININ OXIDASE/DEHYDROGENASE4 integrates cytokinin and auxin signaling to control rice crown root formation, Plant Physiol. 165 (2014) 1035–1046. https://doi.org/10.1104/pp.114.238584.

[33] B.R. Debi, S. Taketa, M. Ichii, Cytokinin inhibits lateral root initiation but stimulates lateral root elongation in rice (Oryza sativa), J. Plant Physiol. 162 (2005) 507–515. https://doi.org/10.1016/j.jplph.2004.08.007.

[34] N. Burman, A. Bhatnagar, J.P. Khurana, OsbZIP48, a HY5 transcription factor Ortholog, exerts pleiotropic effects in light-regulated development, Plant Physiol. 176 (2018) 1262–1285. https://doi.org/10.1104/pp.17.00478.

[35] S. Mcqueen-Mason, D.J. Cosgrove, Disruption of hydrogen bonding between plant cell wall polymers by proteins that induce wall extension, Proc. Natl. Acad. Sci. U. S. A. 91 (1994) 6574–6578. https://doi.org/10.1073/pnas.91.14.6574.

[36] J. Che, N. Yamaji, R.F. Shen, J.F. Ma, An Al-inducible expansin gene, OsEXPA10 is involved in root cell elongation of rice, 31 (2016) 132–142. https://doi.org/10.1111/tpj.13237.

[37] Y. Okushima, H. Fukaki, M. Onoda, A. Theologis, M. Tasaka, ARF7 and ARF19 regulate lateral root formation via direct activation of LBD/ASL genes in Arabidopsis, Plant Cell. 19 (2007) 118–130. https://doi.org/10.1105/tpc.106.047761.

600 [38] A. Li, Y. Zhang, X. Wu, W. Tang, R. Wu, Z. Dai, G. Liu, H. Zhang, C. Wu, G. Chen, X. Pan,
601 DH1, a LOB domain-like protein required for glume formation in rice, Plant Mol. Biol. 66
602 (2008) 491–502. https://doi.org/10.1007/s11103-007-9283-3.

603 [39] A.C.W. Oa, H.W. Lee, N.Y. Kim, D.J. Lee, J. Kim, LBD18 / ASL20 Regulates Lateral Root
604 Formation in Combination with LBD16 / ASL18 Downstream of ARF7, 151 (2009) 1377–1389.
605 https://doi.org/10.1104/pp.109.143685.

606 [40] T.I. Baskin, Patterns of root growth acclimation: Constant processes, changing boundaries, Wiley
607 Interdiscip. Rev. Dev. Biol. 2 (2013) 65–73. https://doi.org/10.1002/wdev.94.

608 [41] S. Ubeda-Tomás, F. Federici, I. Casimiro, G.T.S. Beemster, R. Bhalerao, R. Swarup, P. Doerner,
609 J. Haseloff, M.J. Bennett, Gibberellin Signaling in the Endodermis Controls Arabidopsis Root
610 Meristem Size, Curr. Biol. 19 (2009) 1194–1199. https://doi.org/10.1016/j.cub.2009.06.023.

611 [42] D.J. Cosgrove, Plant expansins: Diversity and interactions with plant cell walls, Curr. Opin. Plant
612 Biol. 25 (2015) 162–172. https://doi.org/10.1016/j.pbi.2015.05.014.

613 [43] Y. Wang, N. Ma, S. Qiu, H. Zou, G. Zang, Z. Kang, G. Wang, J. Huang, Regulation of the α-
614 expansin gene OsEXPA8 expression affects root system architecture in transgenic rice plants,
615 Mol. Breed. 34 (2014) 47–57. https://doi.org/10.1007/s11032-014-0016-4.

616 [44] J. Ni, G. Wang, Z. Zhu, H. Zhang, Y. Wu, P. Wu, OsIAA23-mediated auxin signaling defines
617 postembryonic maintenance of QC in rice, Plant J. 68 (2011) 433–442.
618 https://doi.org/10.1111/j.1365-313X.2011.04698.x.

619 [45] T. Oyama, Y. Shimura, K. Okada, The Arabidopsis HY5 gene encodes a bZIP protein that
620 regulates stimulus- induced development of root and hypocotyl, Genes Dev. 11 (1997) 2983–
621 2995. https://doi.org/10.1101/gad.11.22.2983.

622 [46] S.N. Gangappa, J.F. Botto, The Multifaceted Roles of HY5 in Plant Growth and Development,
623 Mol. Plant. 9 (2016) 1353–1365. https://doi.org/10.1016/j.molp.2016.07.002.

624 [47] R. Sibout, P. Sukumar, C. Hettiarachchi, M. Holm, G.K. Muday, C.S. Hardtke, Opposite root
625 growth phenotypes of hy5 versus hy5 hyh mutants correlate with increased constitutive auxin
626 signaling, PLoS Genet. 2 (2006) 1898–1911. https://doi.org/10.1371/journal.pgen.0020202.

627 [48] K. van Gelderen, C. Kang, R. Paalman, D. Keuskamp, S. Hayes, R. Pierik, Far-red light detection
628 in the shoot regulates lateral root development through the HY5 transcription factor, Plant Cell.
629 30 (2018) 101–116. https://doi.org/10.1105/tpc.17.00771.

[49] Y. Zhang, C. Wang, H. Xu, X. Shi, W. Zhen, Z. Hu, J. Huang, Y. Zheng, P. Huang, K.X. Zhang, X. Xiao, X. Hao, X. Wang, C. Zhou, G. Wang, C. Li, L. Zheng, HY5 Contributes to Light-Regulated Root System Architecture Under a Root-Covered Culture System, Front. Plant Sci. 10 (2019) 1–16. https://doi.org/10.3389/fpls.2019.01490.

[50] Y. Sun, Y. Shi, G. Liu, F. Yao, Y. Zhang, Natural variation in the OsbZIP18 promoter contributes to branched-chain amino acid levels in rice, New Phytol. (2020). https://doi.org/10.1111/nph.16800.

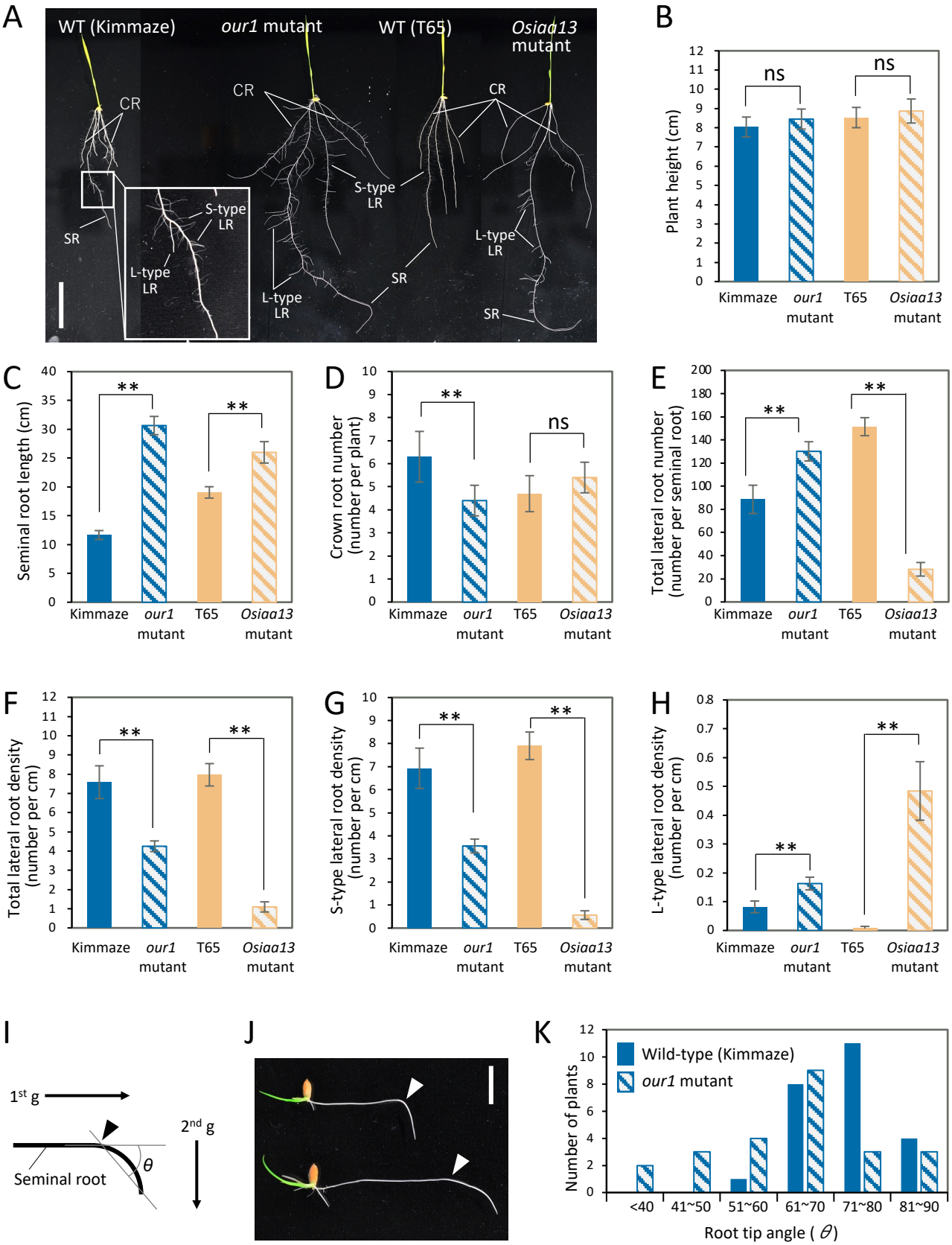
A
WT (Kimmaze)
our1 mutant
WT (T65)
Osiaa13 mutant
CR
SR
S-type LR
L-type LR
B
Plant height (cm)
ns
Kimmaze
our1 mutant
T65
Osiaa13 mutant
C
Seminal root length (cm)
D
Crown root number (number per plant)
E
Total lateral root number (number per seminal root)
F
Total lateral root density (number per cm)
G
S-type lateral root density (number per cm)
H
L-type lateral root density (number per cm)
I
1st g
2nd g
Seminal root
θ
J
K
Wild-type (Kimmaze)
our1 mutant
Number of plants
<40
41~50
51~60
61~70
71~80
81~90
Root tip angle (θ)

Fig. 1

A

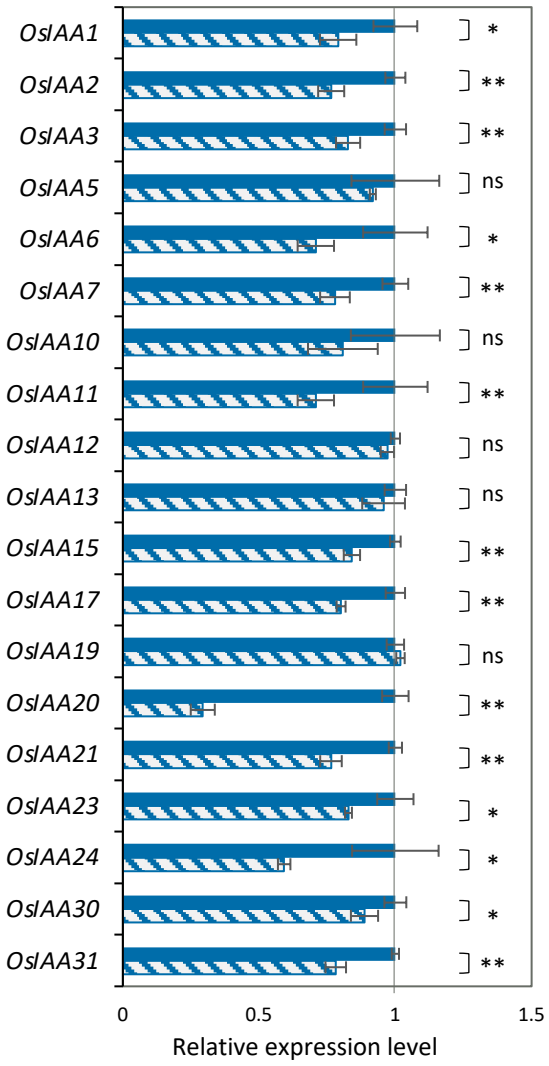
OsIAA1
OsIAA2
OsIAA3
OsIAA5
OsIAA6
OsIAA7
OsIAA10
OsIAA11
OsIAA12
OsIAA13
OsIAA15
OsIAA17
OsIAA19
OsIAA20
OsIAA21
OsIAA23
OsIAA24
OsIAA30
OsIAA31
*
**
**
ns
*
**
ns
**
ns
ns
**
**
ns
**
**
*
*
*
**
0
0.5
1
1.5
Relative expression level

B

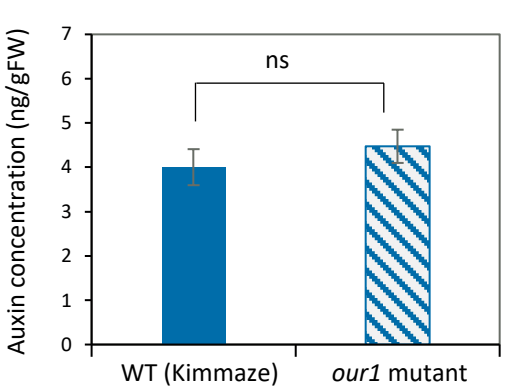
Auxin concentration (ng/gFW)
7
6
5
4
3
2
1
0
ns
WT (Kimmaze)
our1 mutant

Fig. 2

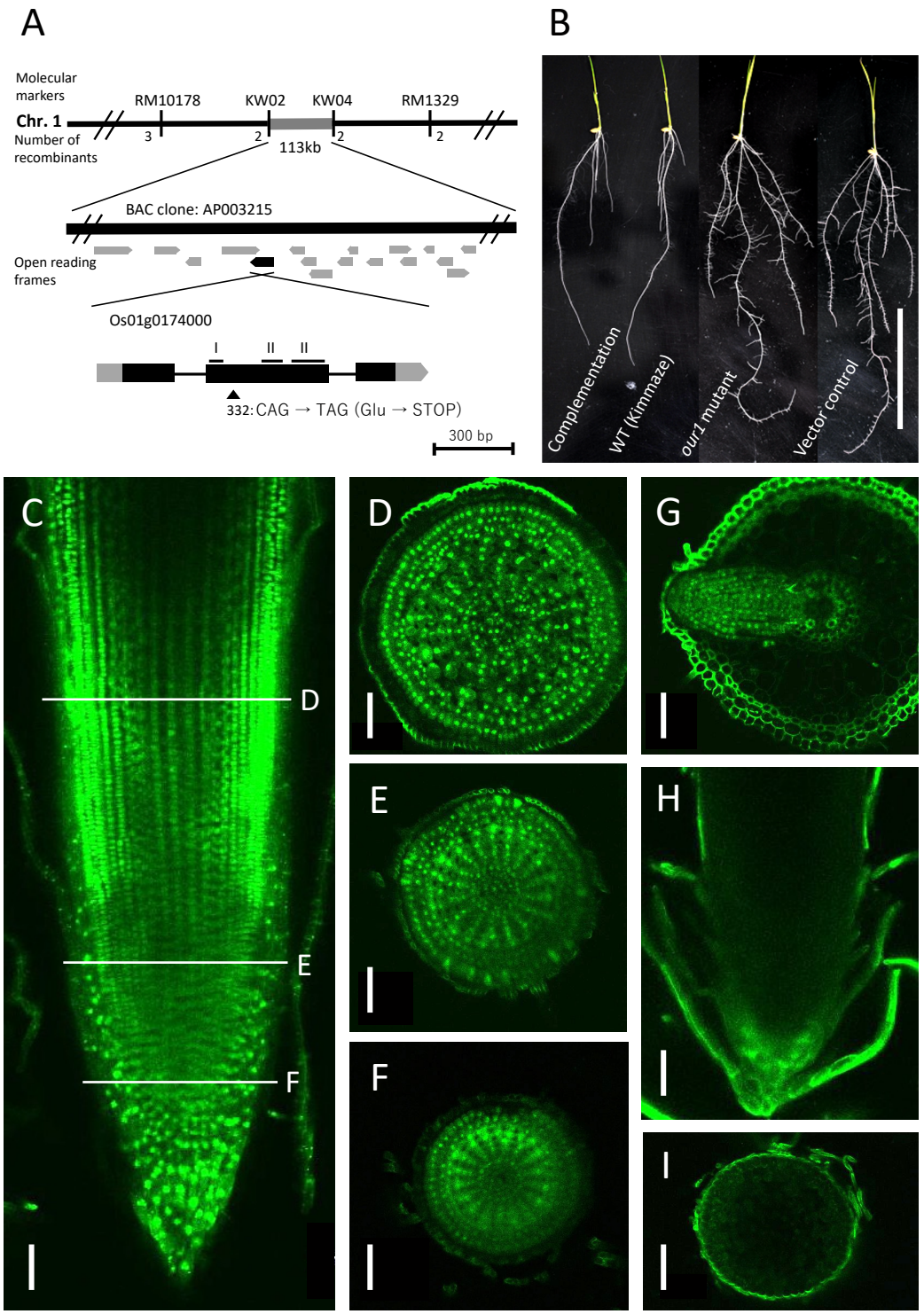
A
Molecular markers
RM10178
KW02
KW04
RM1329
Chr. 1
Number of recombinants
3
2
2
2
113kb
BAC clone: AP003215
Open reading frames
Os01g0174000
I
II
II
332: CAG → TAG (Glu → STOP)
300 bp
B
Complementation
WT (Kimmaze)
our1 mutant
Vector control
C
D
E
F
D
E
F
G
H
I

Fig. 3

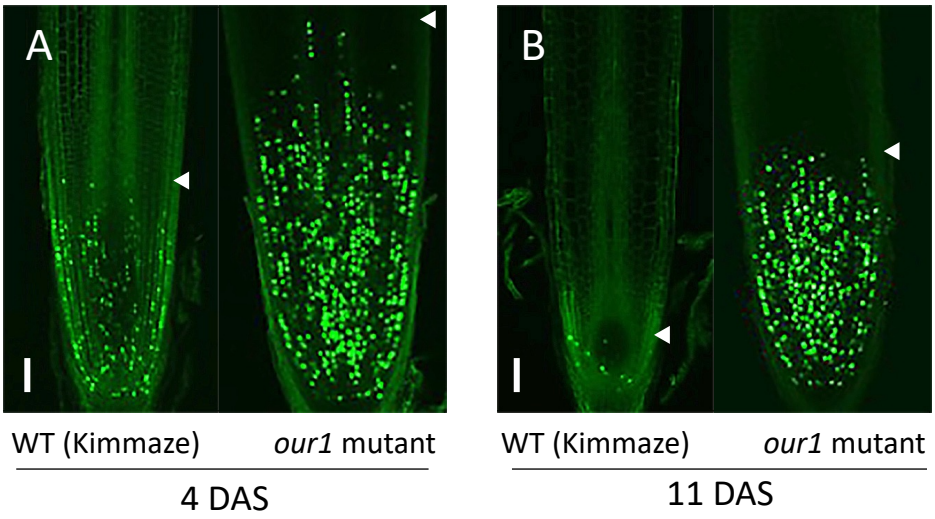
A
B
WT (Kimmaze)
our1 mutant
4 DAS
WT (Kimmaze)
our1 mutant
11 DAS

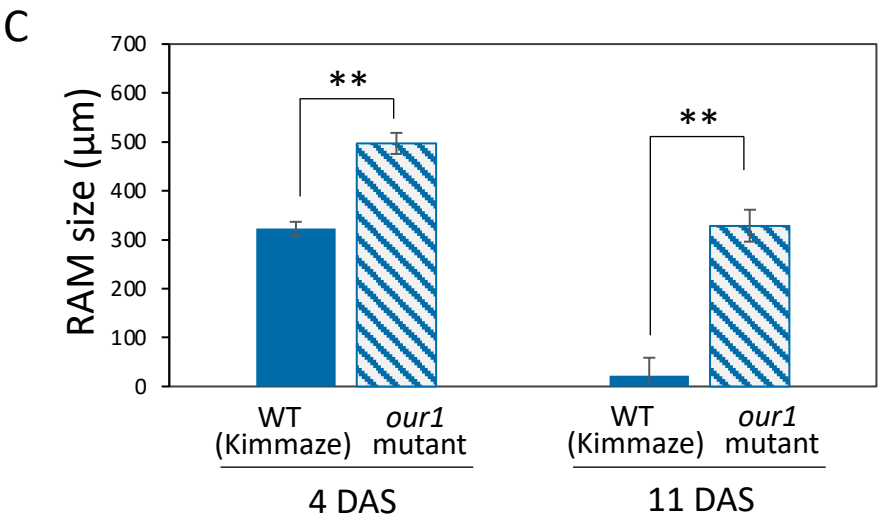
C
RAM size (µm)
700
600
500
400
300
200
100
0
**
**
WT (Kimmaze)
our1 mutant
WT (Kimmaze)
our1 mutant
4 DAS
11 DAS

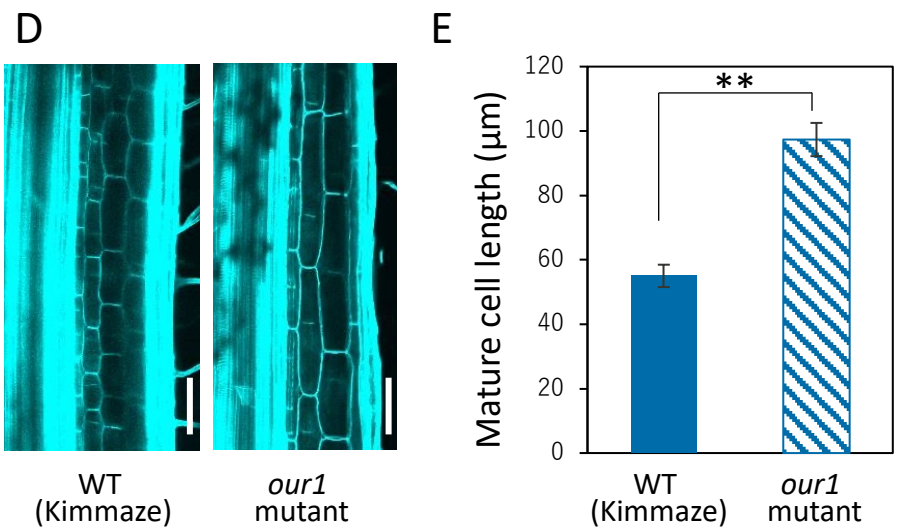
D
E
Mature cell length (µm)
120
100
80
60
40
20
0
**
WT (Kimmaze)
our1 mutant
WT (Kimmaze)
our1 mutant

Fig. 4

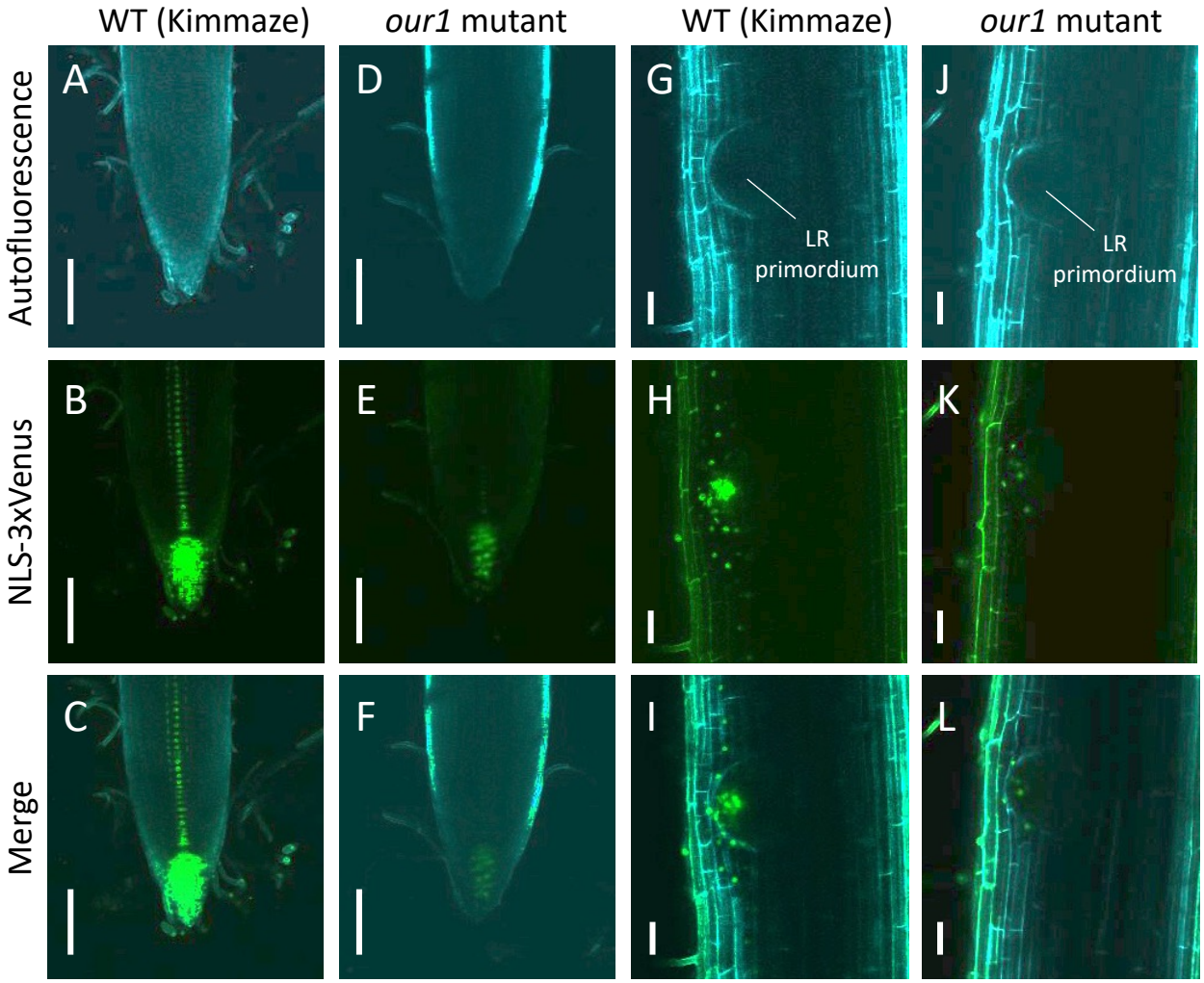
WT (Kimmaze)
our1 mutant
WT (Kimmaze)
our1 mutant
Autofluorescence
NLS-3xVenus
Merge
A
B
C
D
E
F
G
H
I
J
K
L
LR primordium
LR primordium

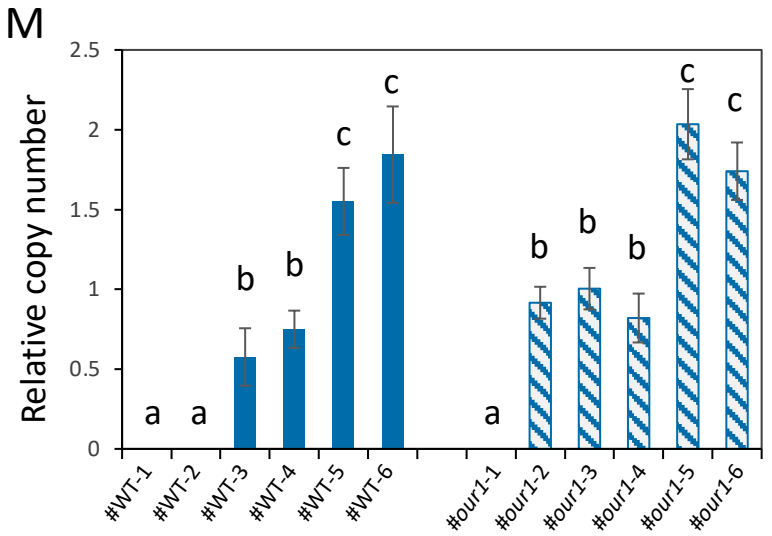
M
Relative copy number
2.5
2
1.5
1
0.5
0
a a b b c c a b b b c c
#WT-1 #WT-2 #WT-3 #WT-4 #WT-5 #WT-6 #our1-1 #our1-2 #our1-3 #our1-4 #our1-5 #our1-6

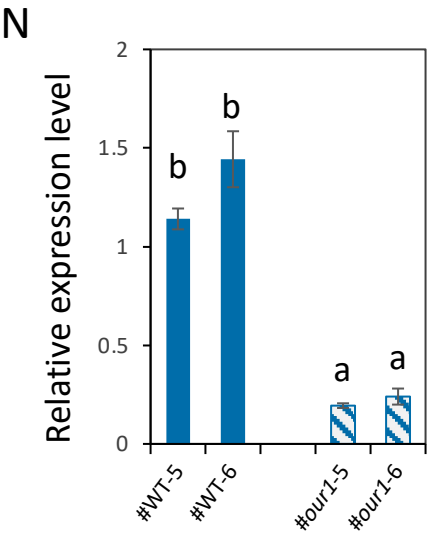
N
Relative expression level
2
1.5
1
0.5
0
b b a a
#WT-5 #WT-6 #our1-5 #our1-6

Fig. 5

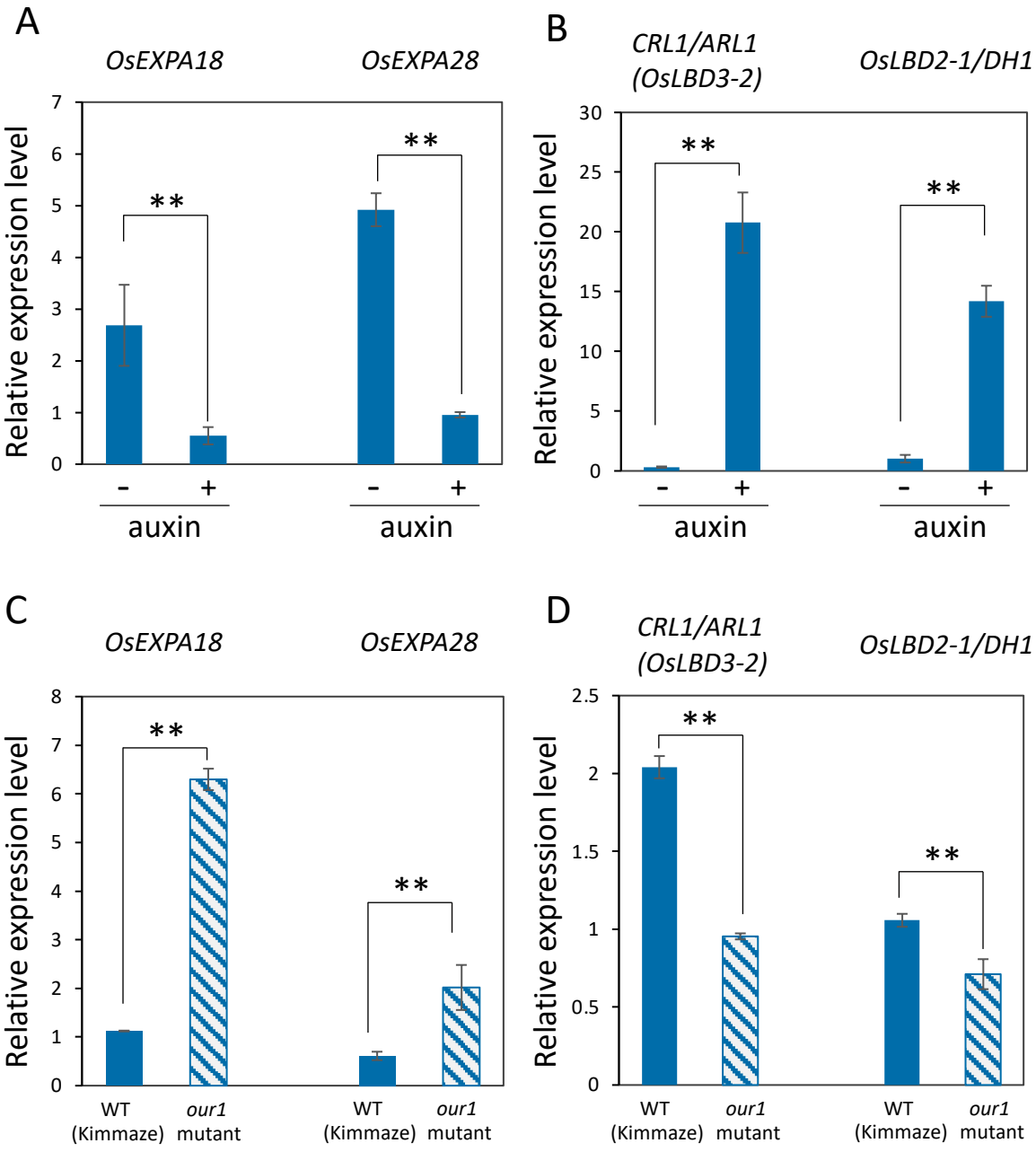
A
OsEXPA18
OsEXPA28
Relative expression level
**
**
- + - +
auxin auxin
B
CRL1/ARL1
(OsLBD3-2)
OsLBD2-1/DH1
Relative expression level
**
**
- + - +
auxin auxin
C
OsEXPA18
OsEXPA28
Relative expression level
**
**
WT (Kimmaze) our1 mutant WT (Kimmaze) our1 mutant
D
CRL1/ARL1
(OsLBD3-2)
OsLBD2-1/DH1
Relative expression level
**
**
WT (Kimmaze) our1 mutant WT (Kimmaze) our1 mutant

Fig. 6